

### Supporting information

#### 1. The image of the ring formation

We increased the thickness of the layer in order to obtain the TEM image of the nanovoid structure clearly. It seemed that very serious aggregation occurred in this sample, but we obtained a relative clear image of this structure.

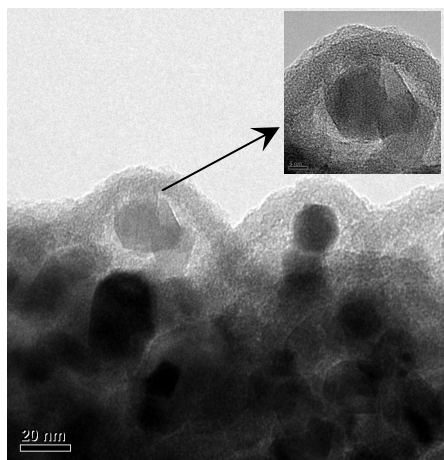
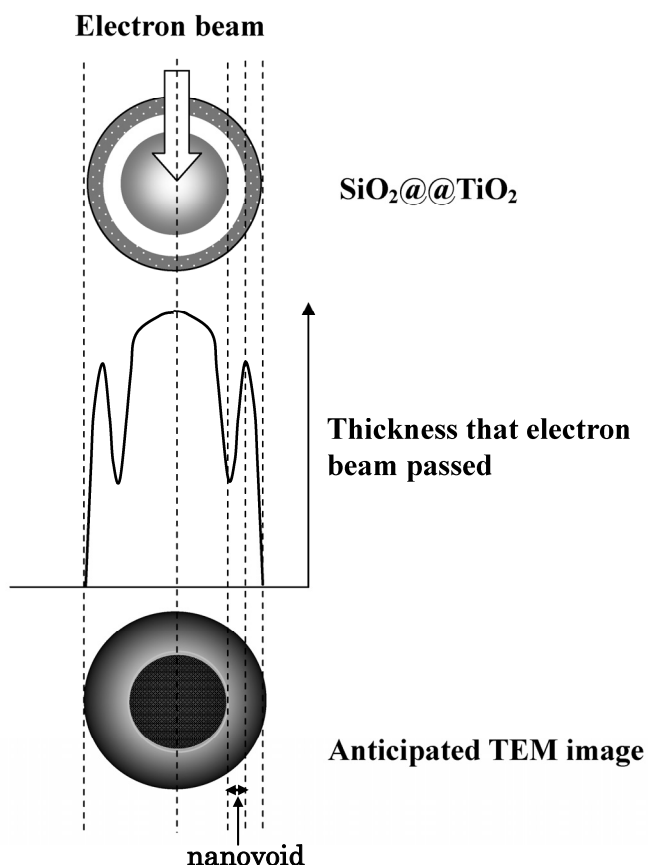


Fig. 1 TEM image of  $\text{SiO}_2@@ \text{TiO}_2$ .

#### Anticipated TEM image of $\text{SiO}_2@@ \text{TiO}_2$ nanoparticles:



**Scheme 1.** Anticipated TEM image of  $\text{SiO}_2@@ \text{TiO}_2$  nanoparticle. Based on the principle of TEM, and data of EDXA, the bright ring in TEM image should show the lowest concentration of Si element adjacent to the  $\text{TiO}_2$  core. Thus we think the bright ring is just a part of the nanovoid structure.

## 2. XRD data

XRD patterns of samples showed there is no obvious anatase-to-rutile phase transformation in SiO<sub>2</sub>@@TiO<sub>2</sub> after calcinations (773K). The result indicates the TiO<sub>2</sub> core can keep as the P-25 phase after the treatment process. (Fig. 2)

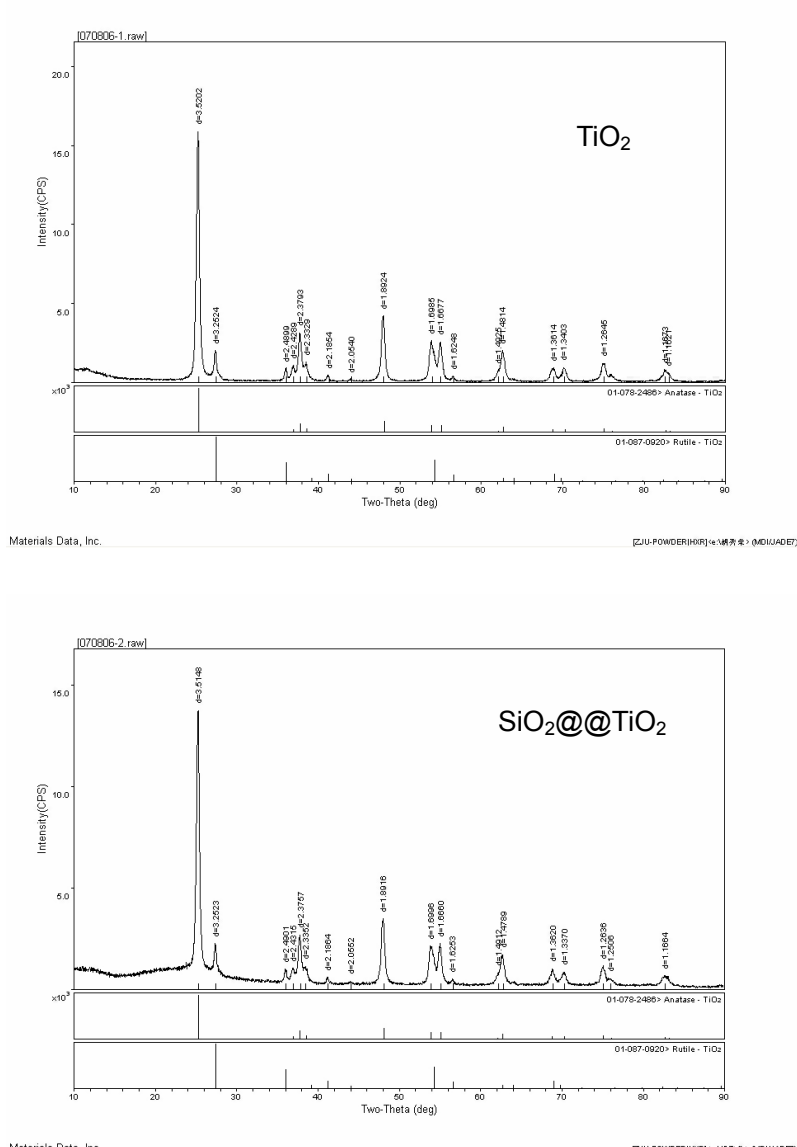


Fig. 2 XRD patterns of TiO<sub>2</sub> and SiO<sub>2</sub>@@TiO<sub>2</sub> nanoparticles.

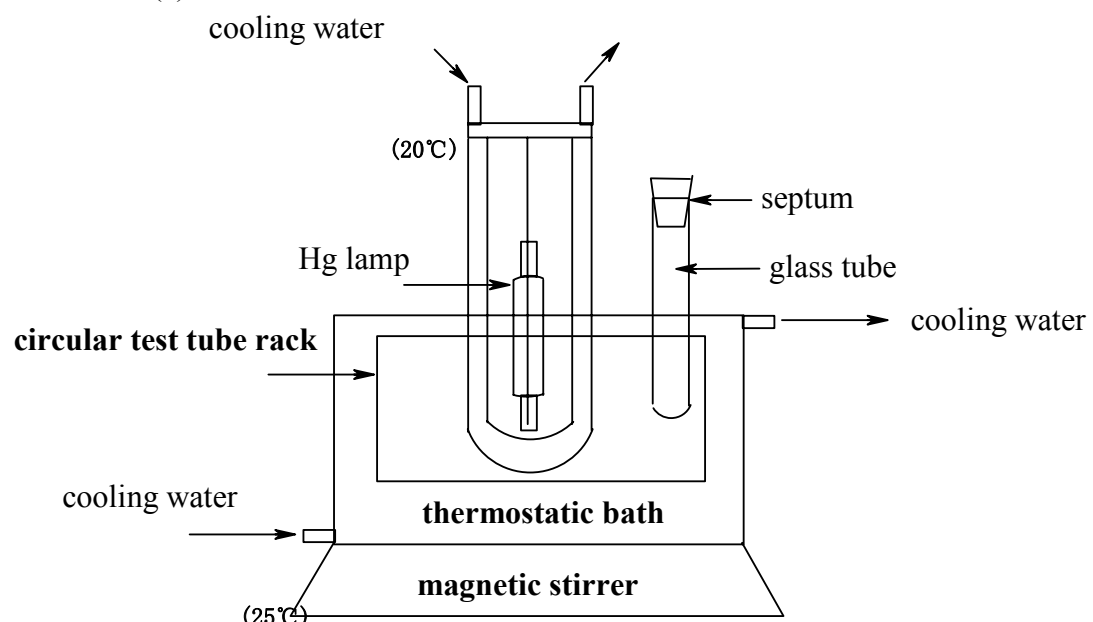
## 3. ICP determination:

The mixture of SiO<sub>2</sub>@@TiO<sub>2</sub> 40 mg, K<sub>2</sub>S<sub>2</sub>O<sub>7</sub> 1.5 g, Na<sub>2</sub>CO<sub>3</sub> 2.5 g and K<sub>2</sub>CO<sub>3</sub> 1.0 g was set in platinum crucible and calcined at 1283K for 20 minutes. Then the melted mixture was cooled down to RT. 300 ml sulfuric acid (VH<sub>2</sub>SO<sub>4</sub> /Vmill-Q=1:9) was used to dissolve this melted mixture. The solution was finally neutralized and adjusted to 1×10<sup>4</sup> ml for ICP determination.

#### 4. Photocatalytic reactor:

A photocatalytic reactor (Nanjing Xujiang Co., Ltd) was used in this study and the schematic details are depicted in Fig. 3. An ultrahigh-pressure Hg lamp (500 W) was located in the center of the reactor along the axis and protected by a water-cooled quartz jacket. At the bottom of the reactor a magnetic stirrer was used to achieve effective dispersion agitating mechanically. A circular test tube rack was inserted on the thermostatic bath to hold up the Pyrex glass tubes. Thus the UV light was collected into the glass tube and ensured the photocatalytic reaction performed uniformly and completely. The reactor was fitted with a magnetic stirrer for stirring at 700 rpm to keep the catalyst in suspension.

(a)



(b)

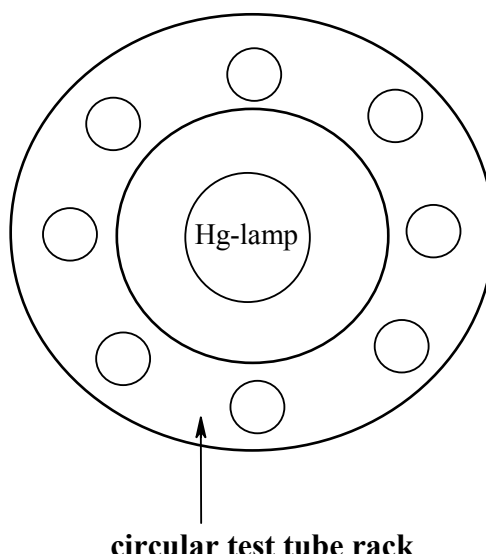
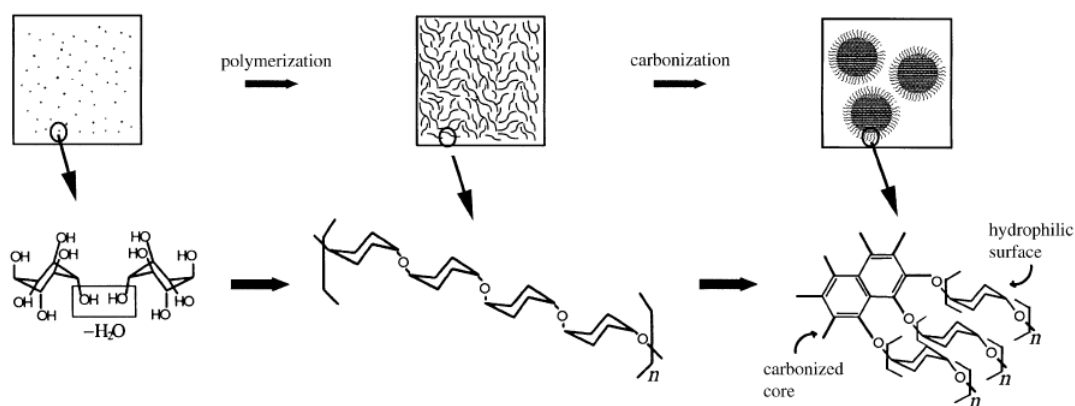


Fig3 Schematic illustration of the cylindrical photocatalytic reactor  
(a) cross-sectional view, (b) top view.

## 5. LaMer model

We think that the porosity of the SiO<sub>2</sub> shell was increased in our experiments. The reason is, during the combustion of the carbon layer, CO<sub>2</sub> had to pass through the SiO<sub>2</sub> layer to get outside. So we think this process is benefit to form the porosity structure of the SiO<sub>2</sub> shell.



However, we think the most important reason own to the following: The growth of the carbon layer, which formed from the hydrothermal process, conform to the LaMer model (*Angew. Chem. Int. Ed.* 2004, 43, 597–601). This model indicates the carbon layer cover around the TiO<sub>2</sub> core closely and successively. That is, in this structure the SiO<sub>2</sub> shell and the TiO<sub>2</sub> core was completely separated by the carbon layer. Thus, we consider that after the combustion process, the nanovoid is formed and the activity sites on the surface of the TiO<sub>2</sub> core are increased by this structure.

## **6. Preparation of $\text{SiO}_2@ \text{TiO}_2$ (or $\text{TiO}_2$ ) immobilized PET fibers:**

First aqueous dispersion of  $\text{SiO}_2@{\text{@}}\text{@}\text{TiO}_2$  was prepared by mixing 0.08 g of  $\text{SiO}_2@{\text{@}}\text{@}\text{TiO}_2$  powder and appropriate amounts of mixture of mill-Q and ethanol ( $\text{V}_{\text{mill-Q}}/\text{V}_{\text{ethanol}}=1:1$ ) in an ultrasonic mixer. PET fibers were treated by base deweighting finishing (with 1 M NaOH at 368K for 30 minutes). Then followed the padding process. Padding process consists of contacting the PET fibers with the padding solution (usually by immersion) and squeezing the padding solution out with squeeze rolls. In this study, the PET fibers were padded for three times with  $\text{SiO}_2@{\text{@}}\text{@}\text{TiO}_2$  aqueous dispersion on a laboratory padding mangle. Finally  $\text{SiO}_2@{\text{@}}\text{@}\text{TiO}_2$  immobilized PET fibers were washed with water for several times, air-dried in an oven (373K for 6 minutes and 453K for 6 minutes).

TiO<sub>2</sub> immobilized PET fibers were prepared according to the procedures that mentioned above and all of the samples were ensured to have the equimolar amounts of TiO<sub>2</sub>.

**7. Photocatalytic decomposition of gaseous formaldehyde by  $\text{SiO}_2@@\text{TiO}_2$  immobilized PET fibers:**

Blank test was first performed by inserting a mount of  $\text{SiO}_2@@\text{TiO}_2$  immobilized PET fibers into a Pyrex glass tube. The tube was then sealed by silicone stopper. This closed system was placed into a photocatalytic reactor, and the concentration analysis of carbon dioxide was conducted with GC.

Photocatalytic decomposition of gaseous formaldehyde by  $\text{SiO}_2@@\text{TiO}_2$  immobilized PET fibers was carried out by injecting a small amount of formaldehyde (0.1 ml) with a syringe into the above closed system. The formaldehyde vapor was allowed to reach adsorption–desorption equilibrium with catalysts in the system prior to UV light irradiation. The concentration analysis of carbon dioxide was conducted with GC.

## 8. The SEM images of PET samples:

The surface morphologies of PET samples were observed by SEM determination.

**Fig. 4a:** The smooth surface of the PET fibers.

**Fig. 4b:** After the base deweighting finishing process, the surface of the PET fibers became rough.

**Fig. 4c:** The surface of the  $\text{TiO}_2$ -immobilized PET fibers after padding process.

**Fig. 4d:** The surface of the  $\text{SiO}_2@@\text{TiO}_2$ -immobilized PET fibers after padding process.

**Fig. 4e:** After 18 h UV irradiation, the cracks and crevasses were observed on the surface of the  $\text{TiO}_2$ -immobilized PET fibers.

**Fig. 4f:** After 18 h UV irradiation, no obvious cracks were observed on the surface of  $\text{SiO}_2@@\text{TiO}_2$ -immobilized PET fibers

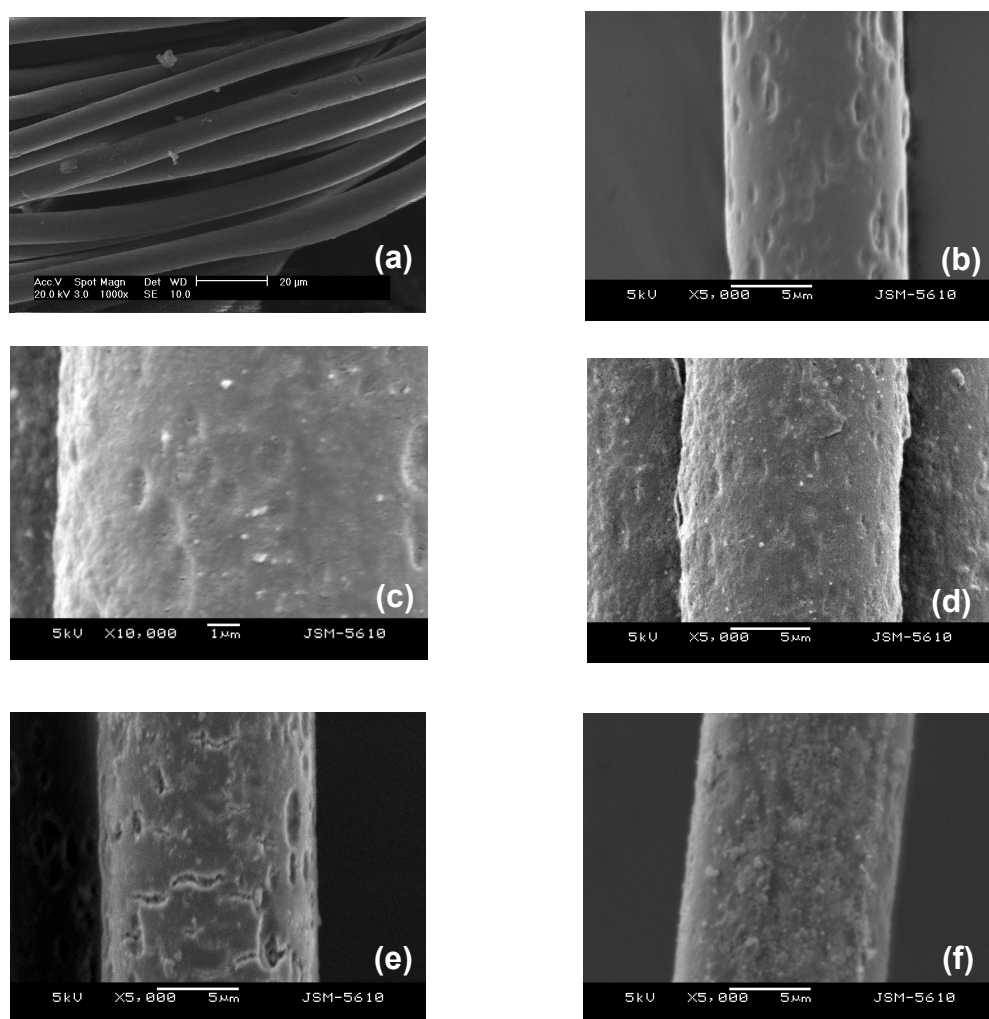


Fig. 4 SEM images of PET fibers.